


Effect of Critical Factors Influencing Longitudinal Track Resistance Leveraging Field Experimentation

Transportation Research Record
1–10
© National Academy of Sciences:
Transportation Research Board 2023
Article reuse guidelines:
sagepub.com/journals-permissions
DOI: 10.1177/03611981231187641
journals.sagepub.com/home/trr


Marcus S. Dersch¹ , Max Potvin¹, Arthur de O. Lima¹ ,
and J. Riley Edwards¹ 

Abstract

As extreme temperatures increase, there is an increased need to ensure that continuous welded rail (CWR) stresses are more accurately set and better maintained. Therefore, to improve the management of CWR rail stresses and to increase safety through the reduction of buckled track derailments this paper documents the results from a field experimentation program of controlled single rail breaks (SRBs). SRBs were conducted at multiple field site locations to quantify the longitudinal resistance on both timber and concrete sleeper track. Accurate longitudinal resistance values are critical, because if the wrong value is selected, the rail neutral temperature could easily be set to a low value, increasing the probability of a track buckle or rail pull-apart, further compounding the impact of extreme temperatures. The results presented quantify the effect of sleeper and fastener type as well as ballast consolidation, and compare them with relevant results from the literature. From this, it was found that well-maintained concrete sleeper track exhibited a longitudinal resistance greater than the currently recommended value. Further, well-maintained timber sleeper track with anchors on every other sleeper exhibited a longitudinal resistance 44% lower than concrete sleeper track and 30% lower than timber track with anchors installed on every sleeper. Additionally, disturbing the ballast reduced the longitudinal resistance by 15%. Finally, the results indicated that slip was primarily occurring at the rail–sleeper interface for unanchored timber sleepers and at the sleeper–ballast interface for anchored timber sleepers and concrete sleepers.

Keywords

ballast, freight rail transportation, railroad infrastructure maintenance, CWR, RNT, SFT

Demands placed on continuous welded rail (CWR) track have increased over recent decades (e.g., greater magnitude temperature swings resulting from more extreme temperatures [1], longer trains which could increase rail temperatures, as well as heavier trains). To accommodate these increased demands, address uncertainty, and improve safety by reducing the occurrence of rail buckle derailments, researchers have performed track panel pull tests (TPPTs) to quantify track longitudinal resistance and stiffness (2–6); Potvin et al. summarized the findings from these, as well as other researchers (6). Longitudinal resistance and stiffness are critical parameters for accurately quantifying the longitudinal loads placed on the track structure components (e.g., fastening systems, sleepers, ballast) and adequately maintaining the longitudinal rail stresses. However, given that TPPTs do not

account for fastener torsional resistance or accurately represent the dynamics of a rail break, and although TPPT values are useful for quantifying load propagation, they are not representative of the resistance values that occur when a rail breaks owing to excess tension or is cut for planned rail stress maintenance (6). In these instances, a single rail break (SRB) test is required to accurately quantify the resistance. For example, Samavedam et al. (7) and Dersch et al. (5) quantified the effect of anchoring pattern on longitudinal resistance using an SRB and

¹Department of Civil and Environmental Engineering, Grainger College of Engineering, University of Illinois at Urbana-Champaign, Urbana, IL

Corresponding Author:

Marcus S. Dersch, mdersch2@illinois.edu

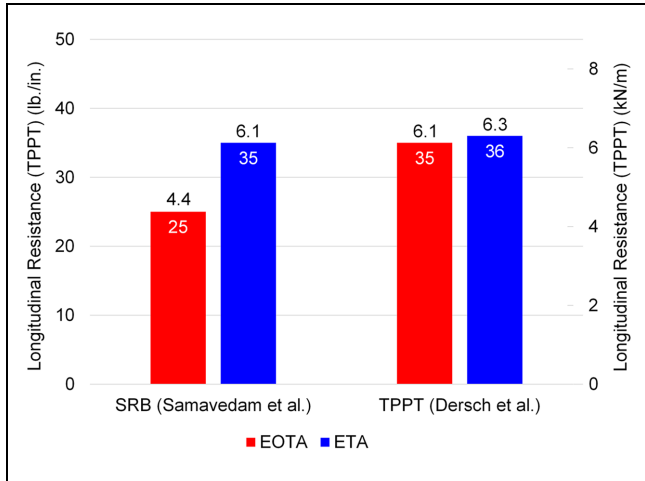


Figure 1. Comparison of longitudinal resistance values as reported by Samavedam et al. (7) and Dersch et al. (5) when changing anchoring pattern leveraging SRBs in the field and TPPTs in the lab, respectively.

Note: SRBs = single rail breaks; TPPTs = track panel pull tests; EOTA = every other sleeper anchored; ETA = every sleeper anchored.

TPPT, respectively. Samavedam et al. found that doubling the number of anchors (i.e., from every other sleeper anchored [EOTA] to every sleeper anchored [ETA]) increased the resistance by approximately 50% when leveraging the SRB test (7), whereas Dersch et al. found negligible change investigating the same using the TPPT (5) (Figure 1).

Samavedam et al. performed the only known SRB experiments before the present study (7). Their experiments were executed to quantify the effect of load magnitude and fastener condition on longitudinal resistance. The results have been used by U.S. railroads and have informed des-tressing operations to this day in that, given a longitudinal resistance, the required number of fasteners to be removed can be more accurately determined. These experiments were performed on a test track at the Transportation Technology Center (TTC) in Pueblo, CO, United States.

However, despite this work, between 2006 and 2015, buckled track still posed the third greatest derailment risk to railroads (8). This indicates that there is room for improvement in the rail stress management practices of railroads and a need for additional clarity in longitudinal resistance values for different track scenarios. Additionally, over this same time-period, broken rails or welds were the most frequent mainline derailment cause with the greatest risk posed to North American railroads (8). Although not every broken rail is caused by improper rail stress management, every rail that breaks, or is cut to remove a defect, will require its rail neutral temperature (RNT), known as the stress free temperature or the temperature at which point there is zero axial (longitudinal) stress in the rail, to be restored.

To manage their longitudinal rail stresses many North American railroads rely on rail adjustment tables or software such as CWR-SAFE (9). Their rail stress management process can be classified as either reactive or proactive. Reactive management means that RNT is restored by the railroad after a rail break. Proactive management indicates that the railroad intentionally removes or adds rail to a given location to change the stress state; typically around fixed structures and/or as seasons are changing (e.g., moving from spring to summer or from fall to winter). In either case, the railroad personnel relate the temperature differential between the prebreak RNT and the in situ rail temperature to the rail gap present (Equation 1) (7).

$$dT = \sqrt{RM \times f_0 / EA\alpha^2} \quad (1)$$

where

dT = difference between RNT and in situ rail temperature, °C (°F),

RM = rail movement because of a rail break or cut, m (in.),

f_0 = longitudinal track resistance, kN/m (lb/in.),

E = rail's modulus of elasticity, MPa (pounds per square inch [psi]),

A = rail's cross-sectional area, m² (in.²), and

α = rail's coefficient of thermal expansion, m/°C (in./°F).

Inherent in this calculation are the assumptions that the RNT was uniform before the break (or cut) and that the longitudinal resistance was known. However, longitudinal resistance is dependent on the type and health of the sleeper and fastening system (i.e., elastic fasteners versus plates, spikes, and anchors), anchoring pattern, and the condition of the ballast (i.e., full versus half-full cribs and consolidated versus disturbed ballast) (2, 4–6). The following is a single example to quantify the adverse effects of selecting an incorrect longitudinal resistance value when performing RNT maintenance.

This example uses 136 RE rail with an area of $8.6 \times 10^{-3} \text{ m}^2$ (13.32 in.²), a modulus of 200,000 MPa (29,000,000 psi), and coefficient of thermal expansion of $2.97 \times 10^{-8} \text{ m}/^\circ\text{C}$ (0.0000065 in./°F). Given there was a gap of 51 mm (2 in.) in the rail, then if the longitudinal resistance of a timber sleeper, with ETA fasteners and undisturbed ballast track (6.1 kN/m [35 lb/in.]) were used in lieu of the same track with disturbed ballast (4.4 kN/m [25 lb/in.]) (10), there would be a 5.6°C (10°F) difference in the calculated temperature differential (dT) (Figure 2). This, in-turn, would result in the railroad personnel restoring RNT 5.6°C (10°F) lower than the target, thus increasing the probability of future buckling. This difference is further magnified if a larger break occurs, which would be more probable during a winter rail break scenario.

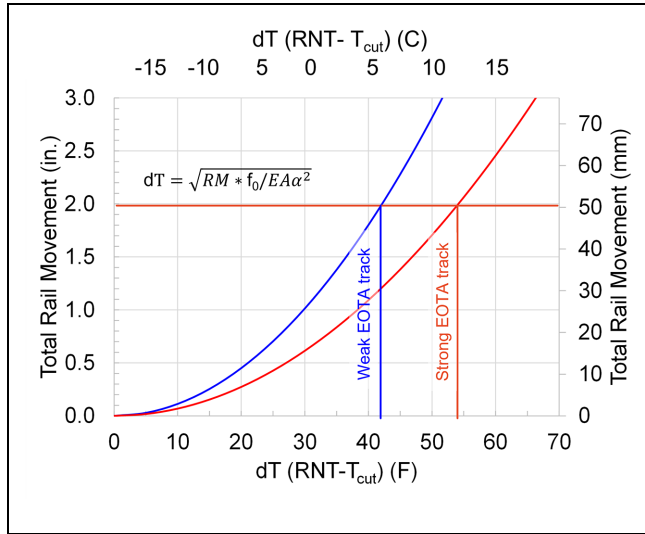


Figure 2. Expected rail movement at various temperature differentials (dT) for weak EOTA (blue) and strong EOTA track (red).
 Note: EOTA = every other sleeper anchored; RNT = rail neutral temperature.

Therefore, this paper documents the results from a field experimentation program of SRBs conducted by the Illinois Rail Transportation and Engineering Center (RailTEC) at multiple locations to quantify the longitudinal resistance on both timber and concrete sleeper track. The results quantify the effect of sleeper and fastener type as well as ballast consolidation and compare them to relevant results from the literature.

Methodology

Single Rail Break Overview

In contrast to TPPTs in which an external load is applied to both rails simultaneously and the panel is pulled through the ballast, an SRB leverages the difference between the RNT and rail cut temperature (dT) to

develop force in a single rail. And whereas TPPTs typically involve applying longitudinal loads to a track panel constructed with 4 to 10 sleepers (2, 11–15), SRBs leverage instrumentation placed over tens of meters (hundreds of feet) to capture the change in force over distance when a rail is cut.

Instrumentation Locations and Site Characteristics

This paper documents SRB experiments that were executed at two different field sites. Site 1 was located on the Facility for Accelerated Service Testing High Tonnage Loop at TTC and both rails were instrumented. Site 2 was located on a heavy axle load (HAL) North American railroad and only a single rail was instrumented. More details about each site and the objectives of the experiments are provided below (Table 1).

All tests were performed on tangent track. However, beyond this, the characteristics of each site were different to quantify the effect of the following track parameters on longitudinal track resistance:

- Sleeper type: concrete and timber;
- Fastening system/anchoring pattern: ETA and EOTA anchoring pattern for timber sleeper track and elastic fasteners (EFs) for the concrete sleeper track; and
- Ballast condition: consolidated and disturbed.

Experimental Matrix and Variables

Six unique tests (rail cuts) were conducted to achieve the aforementioned objectives (Table 2).

Tests 1 and 2 were used to provide confidence in the repeatability of the results. Test 3 was used to quantify the influence (e.g., tamping) disturbing the ballast. Test 4 was used to quantify the effect of different anchoring patterns (i.e., ETA versus EOTA). Finally, Tests 5 and 6 were used to quantify the effect of sleeper type (e.g., concrete sleepers with elastic fasteners [CTEFs]) and provide

Table 1. Single Rail Break Site Characteristics

Details	Site 1 (Rails A and B)	Site 2 (Rail C)
Date	November 2021	April 2022
Geometry	Tangent	Tangent
Crossties	Timber	Concrete
Fastening system	Every other sleeper anchored Every sleeper anchored	Safelok III (EF)
Ballast	Compacted from traffic Disturbed with tamping	Compacted from traffic
Number of tests	4	2
dT (RNT-T _{cut})	~17°C to 22°C (~30°F to 40°F)	~19°C and 36°C (~35°F and 65°F)

Note: EF = elastic fastener; dT = temperature differential; RNT-T_{cut} = rail neutral temperature minus the rail temperature at time of break.

Table 2. Single Rail Break Experimental Matrix at Multiple Sites

Test	Site	Sleeper	Fastener	Rail	Ballast	dT	
						°F	°C
1	1	Timber	EOTA	A	Undisturbed	35	19
2				B		30	17
3				A		30	17
4	2	Concrete	ETA	B	Disturbed	40	22
5				C		35	19
6				EF		65	36

Note: dT = temperature differential; EOTA = every other sleeper anchored; ETA = every sleeper anchored; EF = elastic fastener.

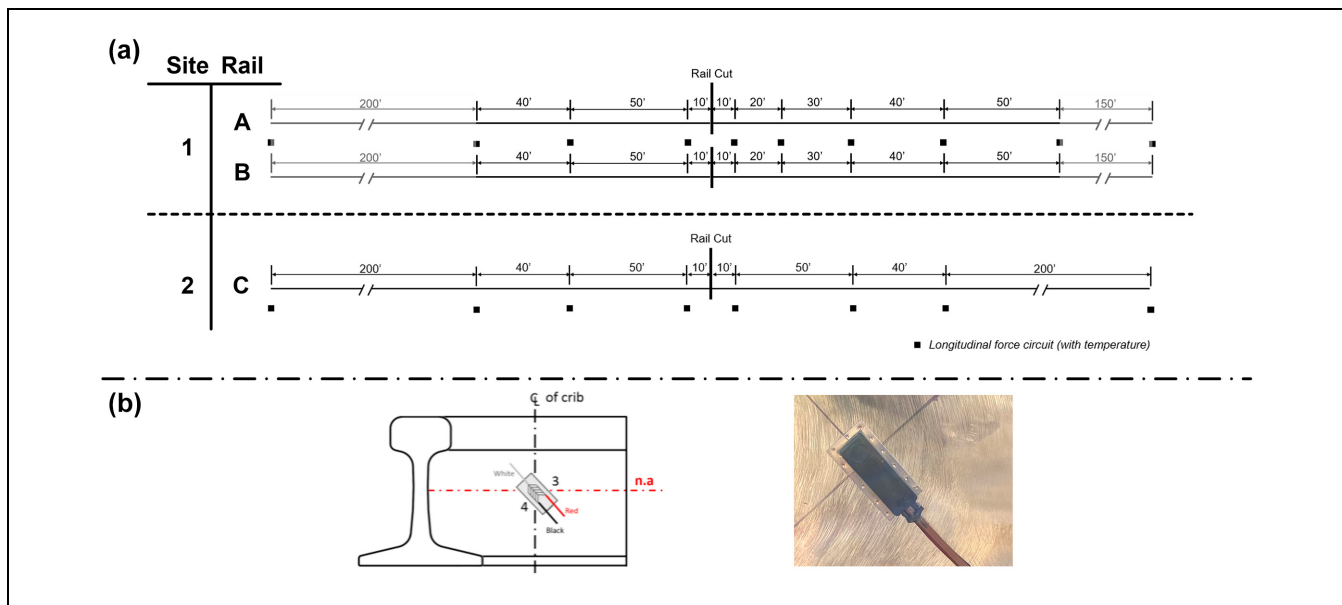


Figure 3. (a) Instrumentation plan for the three rails of both sites and (b) a schematic and example weldable chevron-style strain gauge with built-in thermocouple installed at the neutral axis of the rail.

additional confidence by deploying the same experimental methodology at another unique location.

Rail tensile forces ranging from 330 to 720 kN (75 to 160 kips) were developed by cutting the rail at temperatures that ranged from 17°C to 36°C (30°F to 65°F) below the set RNT. Approximate rail forces can be calculated using Equation 2, with the terms being previously defined.

$$F_{rail} = E \times A \times \alpha \times dT \quad (2)$$

Instrumentation Details

Longitudinal rail stress circuits (Figure 3b) were installed at discrete locations between 3 and 90 m (10 and 300 ft) on either side of the cut at each site (Rails A, B, and C as named in Table 1; see Figure 3a). Ten circuits were installed on both rails of Site 1, whereas eight were

installed on the single rail of Site 2. The circuits were spaced to ensure the change in force from the rail cut could be adequately measured, while also providing redundancy if one of the circuits was damaged.

The theory of how these circuits work has been previously presented by Harrison (16) and Dersch et al. (17). In summary, strain gauges are oriented and wired such that rail bending resulting from lateral loads is canceled. Therefore, these circuits can be used to quantify longitudinal rail loads applied by trains as well as thermally induced longitudinal rail stresses leveraging the Poisson effect of the unconstrained rail in the vertical orientation given a partially or fully constrained rail in the longitudinal direction.

In addition to the deployment of longitudinal circuits, an unmanned aerial vehicle (UAV) was used to provide a qualitative understanding into what track components moved and how much displacement occurred. That is,



Figure 4. Example of a match-mark placed on the rail and plate 83.8 m (275 ft) away from the cut.

the UAV was used to determine where most of the slip occurred (i.e., rail through the fastener or sleeper through the ballast) and whether the behavior was uniform or nonuniform. To improve the accuracy and visualization of the displacement data the commercial digital image correlation (DIC) software package Vic2d was used. And finally, match-marks (Figure 4) were placed on the rails and plates at 7.6 m (25 ft) intervals to provide an additional means of quantifying the relative displacement between the rail and fastener.

Longitudinal Track Resistance Calculations

Longitudinal resistance is defined as the change in force over a given distance of track (Equation 3) for a single rail resulting in units of force per unit of length (e.g., kN/m [lb/in.]). For this study, care was taken to establish a relatively uniform pre-cut RNT through the test zone and, thus, the slope of the in situ force over distance before the rail cut (λ) was taken as zero in most cases. If the slope could not be taken as zero, the data were discarded to increase confidence in the data collected.

$$f_o = (m - \lambda) \tag{3}$$

where

f_o = longitudinal resistance,

m = slope of the change in force over distance from longitudinal rail circuits, and

λ = slope of the in situ force over distance before the rail break.

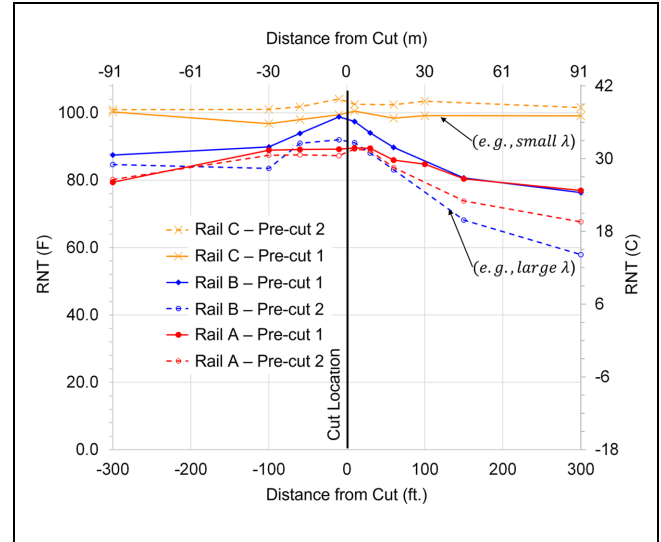


Figure 5. Summary of as-set RNT values before a cut over distance for each rail.

Note: RNT = rail neutral temperature.

Experimental Results

As stated, care was taken to establish a uniform RNT before any of the tests. At Site 1, this was accomplished by distressing the rail once, before performing any tests. Before this distressing, rail anchors were removed for approximately 90 m (300 ft) on either side of the cut. Once the rail was free, it was pulled back together, welded, and rail anchors were reinstalled. At Site 2, distressing was also planned, but this time with the fasteners on. After reviewing the data, it was determined that the RNT was already uniform before the distress and the data could be used for analysis, and thus these data were documented as Test 5. A summary of RNT as set for each rail is shown in Figure 5.

The RNT, as set, for Rail C (RC1 and RC2) was certainly more uniform than that of Rails A and B. Further, the RNT to the right of the cut at Site 1 (RA2 and RB2, as shown in Figure 5), tended to decrease by between 12°C and 16°C (18°F and 26°F) before Tests 3 and 4. Therefore, because this would have led to a highly nonuniform force profile before the cut, no longitudinal resistance data were calculated from this side of the rail from RA2 or RB2. This reduction in RNT was hypothesized to be attributed to the curve that was just beyond (i.e., between 15 and 60 m [50 and 200 ft]) the tangent chosen for this study. That is, it was believed that when the rail was cut and anchors removed, the rail moved into the curve, and when the rail was pulled back, some of the the rail stayed in the curve, thus leading to a higher RNT near the cut location and a lower RNT away from it.

Once the instrumentation was installed, RNT was established by the host railroad leveraging North

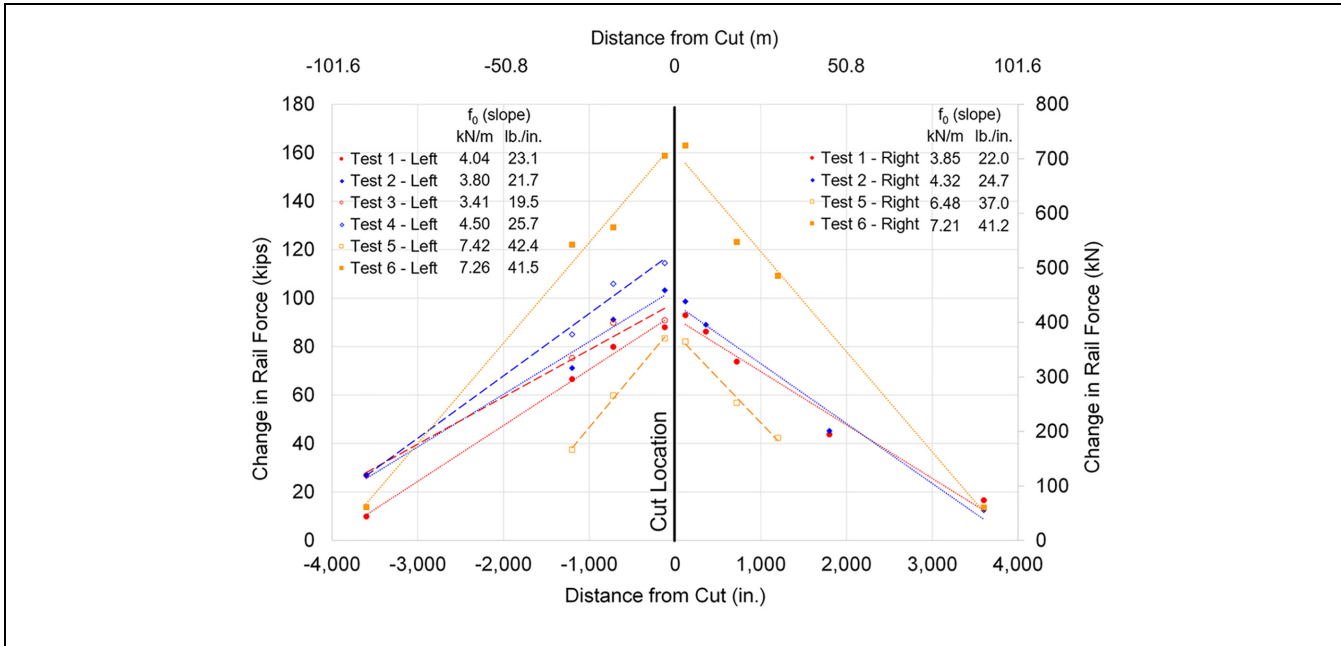


Figure 6. Change in force over distance data, with longitudinal resistance values calculated (i.e., slope [e.g., kN/m (lb./in.)]) for each direction of all tests, with all R^2 values greater than 0.97.

Table 3. Summary of Average Longitudinal Resistance Values for each Condition Tested

Sleeper type	Fastener	Ballast condition	Longitudinal resistance (f_0)	
			kN/m	lb/in.
Timber	EOTA	Undisturbed	4.00	22.9
	EOTA	Disturbed	3.41	19.5
	ETA*	Undisturbed	5.17	29.6
	ETA	Disturbed	4.50	25.7
Concrete	EF	Undisturbed	7.09	40.5

Note: EOTA = every other sleeper anchored; ETA = every sleeper anchored; EF = elastic fastener.

*This condition was not directly tested. Rather the relationship of disturbing ballast with the EOTA condition was applied to the ETA Disturbed ballast test run.

American industry best practices (e.g., leveraging CWR-Safe), and adequate dT was achieved, the rail was cut, and data recorded. And thus, the change in force over distance (Equation 4) for each direction of each rail (except to the right of the cuts for Tests 3 and 4) were calculated (i.e., total of 10 values) and presented (Figure 6). Using a simple linear regression of all change in force over distance data collected at discrete locations, the longitudinal resistance values were also calculated and are documented within Figure 6.

$$\text{Change in Rail Force} = (F_{pre-cut_i} - F_{post-cut_i}) \quad (4)$$

where i = generic location of instrumentation.

The variation in longitudinal resistance (i.e., slope) from one side of the cut to the other among Tests 1, 2, 5, and 6 was less than 10% on average. Further, the longitudinal resistance of replicate tests (e.g., Tests 1 and 2 as well as Tests 5 and 6) were within less than 10% of each other, on average. This provided confidence in the adequacy of the instrumentation and calculation methods given that they were replicates of the same track condition, just on different rails. Further, these values were not expected to be exactly the same, given that longitudinal resistance values are dependent on a variety of factors (e.g., the probability of anchor engagement, plate skew relative to sleeper, changes in sleeper skew). Furthermore, as would be expected, the concrete sleeper track in Tests 5 and 6

exhibited noticeably greater resistance (i.e., greater slope) than all timber sleeper track data. The longitudinal resistance data for each track condition were then averaged for a more detailed comparison (Table 3).

The longitudinal resistance of concrete sleeper track with EF was the greatest measured (7.09 kN/m [40.5 lb/in.]). This value was 11% lower than the median concrete TPPT longitudinal resistance value quantified by Potvin et al. (6). This was not expected given North American concrete sleepers are larger than those used in Europe, which should lead to higher resistance. This provided additional evidence to support the hypothesis that longitudinal resistance values from SRBs should not be conflated with TPPTs.

The timber sleeper track with an EOTA anchor pattern and undisturbed ballast exhibited a longitudinal resistance of 4.01 kN/m (22.9 lb/in.), which was 44% lower than the value for concrete sleeper track. Based on conversations with the industry, EOTA is the most common anchor pattern used with timber sleepers in North America, and timber sleepers make up a significant majority of the track-miles in North America. When the track was tamped, the ballast was disturbed. Disturbing the ballast led to the longitudinal resistance decreasing to 3.41 kN/m (19.5 lb/in.), or by 15%. This value aligns well with the 13% value reported by Dersch et al. using TPPTs (5), but is significantly lower than the 25% reduction median value reported in Potvin et al.'s review of the literature (6). Assuming this 15% value would be consistent for ETA track, the longitudinal resistance of timber sleeper track with an ETA anchor pattern was found to be 5.17 kN/m (29.6 lb/in.), or a 30% increase over the EOTA track condition. This 30% difference indicated that the anchor pattern played a significant role in longitudinal resistance, which is in direct contrast to the TPPT results reported by Potvin et al. (6) and Dersch et al. (5) and consistent with the discussion in the introduction that demonstrated that doubling the number of anchors (e.g., EOTA to ETA) could increase the resistance by 50% (7). Therefore, the data indicated that increasing the number of anchors (e.g., EOTA to ETA) could increase resistance from between 30% to 50%. This is likely driven by the type of anchor, how well the anchor is engaged with the sleeper, and the skew of the plate on the sleeper.

The longitudinal resistance values quantified in this study were compared further with the previous SRB data as recommended by Kish (18; see Figure 7). Before Kish (18), Samavedam et al. had undertaken the only other SRB tests: to determine how track would perform when well-maintained (strong track) and when maintenance was lacking (e.g., anchors not engaged with the sleepers and ballast disturbed: weak track) (7). The authors understand that North American HAL railroads currently leverage the values presented by Kish (18).

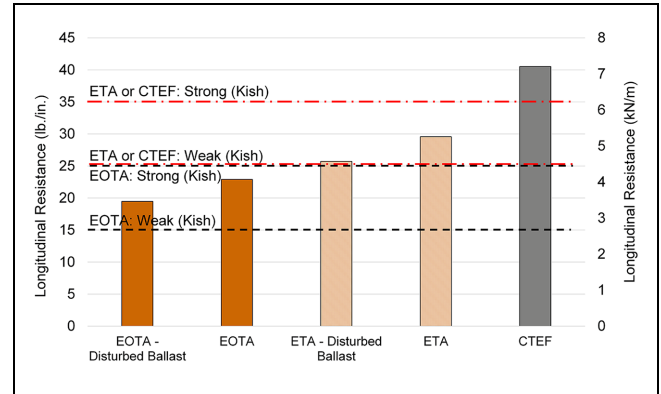


Figure 7. Comparison of longitudinal resistance values from single rail breaks from this study and previous SRB recommended values by Kish (18).

Note: EOTA = every other sleeper anchored; ETA = every sleeper anchored; CTEF = concrete sleepers with elastic fastener.

Most values recorded fell within the range recommended by Kish (18). The one exception was the concrete sleeper resistance. The 7.09 kN/m (40.5 lb/in.) recorded value in this study was approximately 15% greater than that recommended by Kish (6.13 kN/m [35 lb/in.]) (18). Further, the EOTA timber sleeper track appeared to be closer to “strong” track, which aligned with expectations given the Site 1 characteristics and care taken to improve the probability of anchor engagement. Further, the disturbed ballast EOTA track was still not at the bottom of Kish’s recommended floor of 2.63 kN/m (15 lb/in.) (18). It is hypothesized that this value could be achieved if more anchors were disengaged from the sleepers or the crib ballast level was reduced. Furthermore, the ETA track was found to be in the middle of Kish’s recommended range (18). Therefore, although the recommendations for EOTA track appeared reasonable, the upper range for concrete sleeper track should be increased to at least 7 kN/m (40 lb/in.), if not higher, and the lower range for ETA track with disturbed ballast could be lowered to 3.5 kN/m (20 lb/in.) to account for instances in which crib ballast could be lower than designed.

To characterize component displacements at each site, aerial images were captured and match-mark movement was recorded immediately before and after several of the cuts. The following are representative findings from both data sets to better characterize the differences between timber and concrete sleeper track behavior and identify the primary slip interface (e.g., rail through fastener or sleeper through ballast). Qualitative displacements recorded from two of the cuts (one from Site 1 and one from Site 2) are shown in Figure 8 using DIC, as discussed previously. Frames compared to quantify the displacements were captured approximately 0.5 s before and after the rail cut.

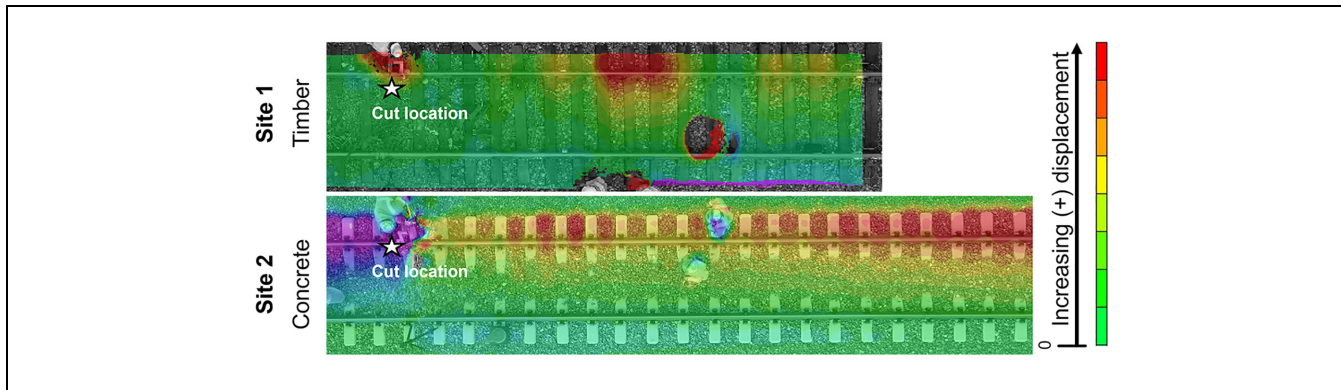


Figure 8. Qualitative comparison of displacements caused by a single rail break on timber and concrete sleeper track.

The Site 1 image is from Test 1 with EOTA and consolidated ballast. The displacement of the sleepers and ballast of the cut rail (i.e., the top rail) was nonuniform. In fact, there were pockets of sleepers that were engaged in load transfer and exhibited larger displacement (red and yellow shades) and pockets in which the sleepers were not engaged in the transfer of load to the ballast (green shades). Once again, this was contrary to the TPPT results Dersch et al. presented (5), but aligns with what Potvin et al. discussed (6). Therefore, when considering timber sleeper track with anchors, the longitudinal resistance was hypothesized to be dependent on the engagement of the anchor with the sleeper (i.e., the longitudinal resistance will be higher when more anchors are engaged). And even when care is taken to properly install an anchor, there is still a possibility that the anchor will not be sufficiently engaged to adequately transfer load.

The Site 2 image is from Test 6 with Safelok III EFs and consolidated ballast. Though harder to tell owing to the person in the middle of the image, the displacements of the sleepers and ballast of the cut rail were more uniform than those seen at Site 1. This aligned with expectations given the probability that all EFs being engaged with the sleepers is greater than anchors with sleepers. Differences in the engagement of EFs could be caused by “sprung” clips (i.e., the toe load has been significantly reduced) or missing clips.

These data also aligned with match-mark data collected, in that they consistently showed that the rail had greater relative movement with the plates on unanchored than with anchored sleepers (Figure 9). The anchored sleepers exhibited some scatter; that is, some locations exhibited more relative movement than others. This is likely caused by a combination of rails slipping through the anchors near the cut, and poor engagement with the sleepers away from the cut (e.g., the data point at 91.4 m [300 ft]).

Additionally, it should be noted that after Test 5, the match-marks placed on the rail and concrete sleepers indicated that nearly all movement was at the sleeper–

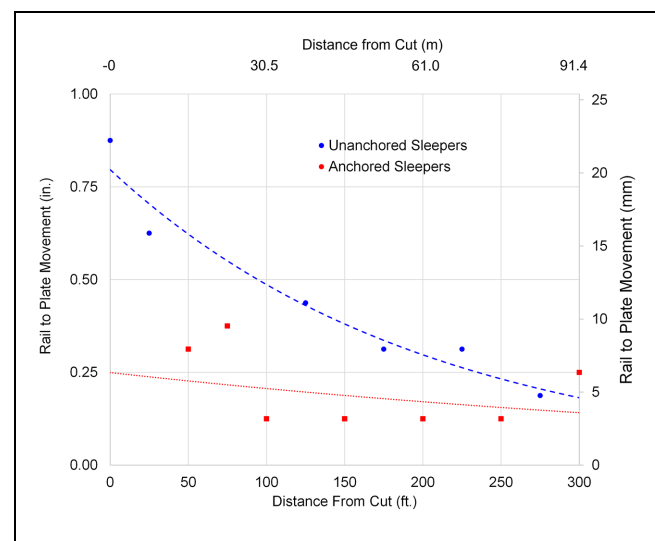


Figure 9. Representative match-mark tracking data for timber sleeper track investigating relative movement between the rail and tie plate of unanchored and anchored sleepers for the right side of the cut.

ballast interface, as opposed to the rail–fastener interface. However, after Test 6, the match-marks closer to the cut location indicated approximately 50% of the displacement was at the rail–fastener displacement and 50% was at the sleeper–ballast interface. Therefore, there is an opportunity to better investigate the mechanics of slip at these interfaces in future experiments.

Conclusions

To improve the management of CWR rail stresses in a global environment experiencing more extreme climate events, and to increase safety through the reduction of buckled track derailments this paper documents the results from a field experimentation program of controlled execution of SRBs. SRBs were conducted at two

field site locations to quantify the longitudinal resistance on both timber and concrete sleeper track. Accurate longitudinal resistance values are critical, because if the wrong value is selected, RNT could easily be set to the wrong value by 5.5°C (10°F), which could increase the probability of a track buckle or rail pull-apart. The results presented quantify the effect of sleeper and fastener type as well as ballast consolidation and compare them with relevant results from the literature.

From this, the following conclusions were made:

- Well-maintained concrete sleeper track exhibited a longitudinal resistance greater than the values recommended by Kish et al. (i.e., 7.09 kN/m [40.5 lb/in.] versus 6.13 kN/m [35 lb/in.]);
- Well-maintained timber sleeper EOTA track exhibited a longitudinal resistance 44% lower than concrete sleeper track;
- Well-maintained timber ETA track exhibited a longitudinal resistance approximately 30% greater than EOTA track;
- Disturbing the ballast via tamping reduced the longitudinal resistance by 15%;
- In contrast to the TPPT results reported in the literature, the SRB results in the literature and in this study indicated EOTA and ETA significantly affected the longitudinal resistance; and
- Slip is primarily occurring:
 - a. At the rail–sleeper interface for unanchored timber sleepers
 - b. At the sleeper–ballast interface for anchored timber sleepers and concrete sleepers.

Therefore, based on these findings, it is recommended that North American railroads select appropriate longitudinal resistance values when managing CWR stress. Specifically, for well-maintained concrete sleeper track, they should consider using up to 7 kN/m (40 lb/in.), whereas the lower expected resistance would be approximately 4.4 kN/m (25 lb/in.). The values presented in this study give additional confidence to the EOTA and ETA values previously presented and continue to encourage the industry to avoid conflating TPPT and SRB results.

Acknowledgments

The authors also would like to acknowledge the following project industry partners for supplying insight, recommendations, and materials to this study: BNSF, Union Pacific Railroad, Amtrak, MxV Rail, and the U.S. DOT Volpe Center. Additional thanks to Andrew Kish for his consultations and insights into the topic of longitudinal resistance and rail neutral temperature and to the Federal Railroad Administration, part of the United States Department of Transportation, for funding the field work and analysis.

Author Contributions

The authors confirm contribution to the paper as follows: study conception and design: Marcus S. Dersch, and J. Riley Edwards; data collection: Max Potvin, Arthur Lima, and Marcus Dersch; analysis and interpretation of results: Marcus Dersch; draft manuscript preparation: Marcus Dersch and J. Riley Edwards. All authors reviewed the results and approved the final version of the manuscript.




Declaration of Conflicting Interests

The authors declared no potential conflicts of interest with respect to the research, authorship, and/or publication of this article.

Funding

The authors disclosed receipt of the following financial support for the research, authorship, and/or publication of this article: This research effort is funded by the Federal Railroad Administration, part of the United States Department of Transportation under the project titled Rail Integrity and RNT Research to Quantify Parameters Influencing Track Longitudinal Stiffness and its Implications for Rail Adjustment Procedures – Phase 2 with contract number 693JJ620C000022. J. Riley Edwards has been supported in part by the grants to the Illinois Rail Transportation and Engineering Center (RailTEC) from CN and Hanson Professional Services.

ORCID iDs

Marcus S. Dersch  <https://orcid.org/0000-0001-9262-3480>
 Arthur de O. Lima  <https://orcid.org/0000-0002-9642-2931>
 J. Riley Edwards  <https://orcid.org/0000-0001-7112-0956>

References

1. Sheridan, S. C., and C. C. Lee. Temporal Trends in Absolute and Relative Extreme Temperature Events Across North America. *Journal of Geophysical Research: Atmospheres*, Vol. 123, No. 21, 2018, pp. 11–889.
2. Zakeri, J. A., and K. Yousefian. Experimental Investigation into the Longitudinal Resistance of Ballasted Railway Track. *Proceedings of the Institution of Mechanical Engineers, Part F: Journal of Rail and Rapid Transit*, Vol. 235, No. 8, 2021, pp. 969–981.
3. Nobakht, S., J. A. Zakeri, and A. Safizadeh. Investigation on Longitudinal Resistance of the Ballasted Railway Track Under Vertical Load. *Construction and Building Materials*, Vol. 317, 2022, p. 126074.
4. Safizadeh, A., J. A. Zakeri, and S. Nobakht. Laboratory Investigation on Contribution of Fastening System and Sleeper in Longitudinal Resistance of Ballasted Railway Tracks. *Road Materials and Pavement Design*, Vol. 24, No. 7, 2023, pp. 1712–1727.
5. Dersch, M. S., M. Potvin, A. D. O. Lima, and J. R. Edwards. Effect of Critical Factors Influencing Longitudinal Track Resistance Leveraging Laboratory Track Panel Pull Test Experimentation. *Transportation Research Record: Journal of the Transportation Research Board*, 2023. 2677.

6. Potvin, M., M. Dersch, J. R. Edwards, and A. D. O. Lima. Review of Critical Factors Influencing Longitudinal Track Resistance. *Transportation Research Record: Journal of the Transportation Research Board*, 2023. 2677: 558–569.
7. Samavedam, G., J. Gomes, A. Kish, and A. Sluz. *Investigation on CWR Longitudinal Restraint Behavior in Winter Rail Break and Summer Destressing Operations*. FRA, Washington, D.C., 1997, p. 74. <https://railroads.dot.gov/elibrary/investigation-cwr-longitudinal-restraint-behavior-winter-rail-break-and-summer-destressing>. Accessed September 24, 2020.
8. Wang, B. Z., C. P. Barkan, and M. Rapik Saat. Quantitative Analysis of Changes in Freight Train Derailment Causes and Rates. *Journal of Transportation Engineering, Part A: Systems*, Vol. 146, No. 11, 2020, p. 04020127.
9. Kish, A., and G. Samavedam. *Risk Analysis Based CWR Track Buckling Safety Evaluations*. US Department of Transportation's Volpe Center, Cambridge, MA, 2001, p. 19.
10. Read, D., and A. Kish. *Rail Neutral Temperature Maintenance Guidelines*. Technology Digest Report No. TD12-026. TTCI, Pueblo, CO, 2012, p. 4.
11. Van 't Zand, J., and J. Moraal. *Ballast Resistance Under Three Dimensional Loading*. Delft University of Technology, 1998. <https://esveld.com/Download/TUD/Ballast%20tests.pdf>. Accessed April 4, 2021.
12. Queiroz, R. C. *Longitudinal Track-Ballast Resistance of Railroad Tracks Considering Four Different Types of Sleepers*. Sao Paulo State University, 2006.
13. Kerokoski, O. Determination of Longitudinal and Transverse Railway Track Resistance. *Proc., Joint Rail Conference*. Urbana, IL, ASMEDC, New York, Vol. 1, 2010, pp. 157–165. <https://asmedigitalcollection.asme.org/JRC/proceedings/JRC2010/49064/157/347184>. Accessed June 12, 2020.
14. De Iorio, A., M. Grasso, F. Penta, G. P. Pucillo, S. Rossi, and M. Testa. On the Ballast–Sleeper Interaction in the Longitudinal and Lateral Directions. *Proceedings of the Institution of Mechanical Engineers, Part F: Journal of Rail and Rapid Transit*, Vol. 232, No. 2, 2018, pp. 620–631.
15. Xiao, J., H. Liu, P. Wang, G. Liu, J. Xu, and R. Chen. Evolution of Longitudinal Resistance Performance of Granular Ballast Track with Durable Dynamic Reciprocated Changes. *Advances in Materials Science and Engineering*, Vol. 2018, 2018, p. 12.
16. Harrison, H. Managing the Longitudinal Forces in Heavy Haul Track. *Proc., International Heavy Haul Association, International Heavy Haul Association (IHHA)*, Brazil, 2005, p. 6.
17. Dersch, M. S., M. Trizotto, J. R. Edwards, and A de Oliveira. Quantification of Vertical, Lateral, and Longitudinal Fastener Demand in Broken Spike Track: Inputs to Mechanistic-Empirical Design. *Proceedings of the Institution of Mechanical Engineers, Part F: Journal of Rail and Rapid Transit*, Vol. 236, No. 5, 2021, pp. 557–569.
18. Kish A. *Track Buckling Prevention and Improved Rail Stress Management*. Track Buckling Prevention Workshop, Colorado Springs, CO, 2019.

The material in this paper represents the position of the authors and not necessarily that of the sponsors.